

Evaluation of Fuel Benefits Depending on Continuous Descent Approach Procedures

Yi Cao, Li Jin, Nguyen V. P. Nguyen, Steven Landry, Dengfeng Sun, and Joseph Post

In this work arrival traffic following a continuous descent approach profile into the Hartsfield-Jackson Atlanta International Airport was simulated based on actual recorded traffic data. The fuel burn for the simulated traffic was estimated using the Base of Aircraft Data (BADA) Thrust Specific Fuel Consumption model and compared to a baseline simulation of the as-flown trajectories, where the continuous descent approach profile was not followed. Several sources of variability that impact the fuel savings were examined, including separation minima, types of maneuver to absorb the delays, and composition of aircraft weight category in the fleet mix. The results indicate that fuel savings depended on a number of factors, including aircraft weight, number of step-downs, and the type of air traffic control maneuver used to impart delay to the aircraft. These effects are estimated using simulation.

INTRODUCTION

Previous studies have indicated that the fuel savings expected to result from arrival aircraft flying an optimized profile descent (OPD) can be neutralized by the need to provide separation assurance [Cao et al. 2011]. As a result, the estimate of fuel savings under high traffic demand, where delays because of separation assurance needs may be high, will be reduced compared to that found under lighter traffic demand conditions. The extent to which this reduction in the benefit of OPDs is exacerbated by separation minima, the types of maneuvers used to absorb delays, traffic demand level, and fleet composition is unknown. Knowledge of the effect of these factors is critical to understanding where and under what conditions OPDs might provide significant fuel benefits.

To address this need, a set of simulation studies was conducted. As input, the simulations used Traffic Flow Management System (TFMS) recordings of arrival traffic into the Hartsfield-Jackson Atlanta International Airport over a 14-day period and involved a National Aeronautics and Space Administration (NASA) simulation tool, the Future ATM Concepts Evaluation Tool (FACET), fuel modeling using EUROCONTROL's Base of Aircraft Data (BADA), simple arrival scheduling that generally followed NASA's Multi-center Traffic Management Advisor (McTMA) scheduling algorithm, and wind information obtained from the NOAA Rapid Update Cycle version 2 (RUC2) dataset. Simulations of traffic flying a particular type of OPD, called a continuous descent approach (CDA), under various conditions were compared with a baseline simulation, where the aircraft flew their trajectories as closely as possible to the recorded, "as-flown" flight paths, which followed the typical "step-down" profile rather than the CDA.

In the next section, background is provided on OPDs, previous work in this area, and the tools used in the research. The methodology is then presented, followed by results, discussion, and conclusions.

BACKGROUND

Optimized profile descents

The desire to reduce the environmental impact of air traffic [Clarke et al., 2004] and concern over uncertainties in the jet fuel market have led to consider making arrival routing more efficient through the use of OPDs, such as CDAs, that seek to reduce the fuel burned during the approach phase of a flight [Shresta et al., 2009]. The various forms of OPDs have been projected to result in significant noise footprint and emission reductions as well as fuel savings. As such, they are considered a promising descent procedure to help alleviate some of the environmental impacts of the aviation industry [Jin et al., 2013].

In a conventional approach profile aircraft usually have multiple level flight segments when approaching the destination airport. These level segments (or level-offs) are required by the air traffic controllers (ATCs) to meet altitude restrictions or speed constraints for coordination or safety assurance. During these level segments, aircraft must increase their throttle to maintain speed and altitude, which increases their fuel burn rate, gas emission rate, and noise footprint over periods where the throttle is reduced. Therefore, avoiding such level segments is expected to lead to a reduction in these undesirable effects.

CDAs are one type of OPD where a pre-defined procedure with a static routing is followed by the arriving aircraft, and in which the aircraft maintains a near-idle throttle setting from top-of-descent (TOD) to a point within several miles of the runway threshold [Clarke, 2006]. (The terms OPD and CDA are sometimes used synonymously.) Other types of OPDs include Tailored Arrivals [Coppenger et al., 2009], where a dynamic, conflict-free routing is uplinked to the aircraft prior to starting the arrival using data communications, and three-dimensional path arrival management (3DPAM) procedures, where CDA procedures are augmented with multiple lateral paths that can be assigned based on the need to deconflict traffic.

Previous work

Considerable research has been done on the operation and benefits of CDAs. The European Commission initiated the Optimized Procedures and Techniques for Improvement of Approach and Landing (OPTIMAL) program in 2004 [de Muijnck, 2007], where two major field tests were reported, one at Amsterdam Airport Schiphol, the Netherlands [Wat et al., 2006], and the other at London Heathrow Airport, the UK [Reynolds et al., 2005]. In the US a program known as Partnership for Air Transportation Noise and Emission Reduction (PARTNER) has conducted extensive simulation-based

research as well as field tests, such as the 2002 Louisville test [Clarke et al., 2004; Clarke, 2006] and the Los Angeles test [White and Clarke, 2006].

All the aforementioned field tests concluded that CDAs lead to fuel savings, noise and emission reduction, and total flight time decreases on an individual flight basis. Other reports, however, show that CDAs potentially decrease an airport's throughput because of the need to buffer separation between aircraft to account for uncertainty regarding future positioning of aircraft pairs. Since modifying an aircraft's speed, route, or altitude after approval of a CDA would severely reduce or even eliminate the benefits of the CDA, the uncertainties in TOD points vary among different aircraft, and uncertainties in the speed profiles tend to accumulate as the aircraft descends. Ren and Clarke [2007] employed a total probability method in spacing analysis to account for the uncertainties in arrival metering. Monte Carlo simulations revealed that the uncertainties could result in decrease in airport throughput [Ren and Clarke, 2008]. Therefore, CDAs are usually used in selected airports during periods of low traffic density. In the Louisville airport trial the CDA procedures were assigned only to UPS aircraft and conducted during nighttime hours. In 2009 a trial at the Atlanta airport considered flights from only Delta Air Lines and AirTran Airways. Similarly, trials at the London Metroplex (Luton, Stansted, Gatwick, and Heathrow) reported benefits based on statistics from nighttime operations only [Reynolds et al., 2005].

Because of the difficulty in testing CDAs under high traffic conditions, simulation-based evaluations were conducted in which spacing and sequencing issues were taken into account. Wilson and Hafner [2005] simulated around 2,800 flights at Hartsfield–Jackson Atlanta International Airport (ATL) using the Total Airport and Airspace Model (TAAM), where altitude and ground track constraints were removed to allow the optimal trajectories. The CDA reportedly increased the occurrence of loss of separation by 10%. Shresta et al. [2009] investigated a full day of traffic data at Denver International Airport and validated a method that solves conflicts between the arrival and departure traffic, but the authors also concluded that some level-offs are inevitable to stagger the arrival and departure flows at different altitudes. Khan et al. [2009] demonstrated an analysis of ground automation impact on the CDA in a high density environment, where merging and spacing commands were issued to the arriving traffic to enable a conflict-free CDA.

To link the optimized descent procedure with the fuel benefits, Robinson and Kamgarpour [2010] used distance-to-fly and time-to-fly constraints to characterize the OPD profiles and estimated the potential fuel savings at the 35 OEP airports in the US. The statistical analysis revealed that the fuel savings because of OPDs (or CDAs) are marginal. The time-constrained scenario partially accounted for the time metering in high traffic conditions, where the fuel benefits are compromised by a 70% to 85% reduction because of prolonged flight distance. A more realistic OPD scenario with specific metering constraints along the arrival routes was established in an Oceanic Tailored Arrivals trial reported by Coppenbarger et al. [2009], where a 25% fuel burn penalty was subtracted from the saving numbers to account for upstream metering actions because of OPD operations. This finding was further verified by a human-in-the-loop OPD arrival simulation in ATL by The MITRE Corporation, where controllers suggested that they

tended to use ten miles-in-trail for separation purposes to account for the variability of TODs during busy traffic. In addition, airport throughput efficiency was traded off, such that only 15% of the benefits are preserved [Johnson, 2009].

As a simulation-based evaluation, this study consists of several components: 1) CDAs simulation, 2) fuel estimation model, 3) inter-arrival deconfliction and 4) en route delay absorptions. The following sections describe each of the modules. A sensitivity study follows to analyze the key factors that influence the fuel benefits. A cross-study comparison is presented followed by concluding remarks.

METHODOLOGY

Dataset

The air traffic used in this study is extracted from the Aircraft Situation Display to Industry (ASDI) data generated by TFMS. ASDI data of arriving traffic into ATL between October 1st and 14th, 2011 were used; the dataset contained complete arrival trajectories for 17,694 aircraft. ASDI data include information on each flight in the US National Airspace System (NAS), including each aircraft's identification, 4-dimensional trajectory, ground speed, aircraft type, origin and destination airports, and flight plans. Also used in this study were corresponding recordings from the NOAA RUC-2, which provides weather information, including winds aloft. The RUC-2 covers the whole NAS, with a horizontal resolution of 40 km per grid and a vertical resolution of 37 isobaric levels ranging from sea level to 53,000 ft above mean sea level (MSL) [Bilimoria et al., 2000]. In addition to wind information the RUC-2 provides temperature and pressure information. The International Standard Atmosphere is assumed for other atmosphere parameters used for fuel burn computations.

Traffic Simulation

To estimate the fuel burn under different conditions, we created three traffic scenarios:

Scenario 1, Step-downs: Radar track data from ASDI serves as the baseline for comparison. The traffic pattern reflects the current flight operations, including the step-down descent that is of typical interest to this research. Given that the recorded arrivals are coordinated by ATCs, the baseline traffic is assumed to be conflict-free.

Scenario 2, CDAs without delays: CDAs are simulated, but conflict detection and resolution (CD&R) is not incorporated. The recorded flights are simulated according to the filed flight plan and aircraft performance data. Specifically, given the aircraft type information, the nominal speed profile pertaining to that aircraft type is used to synthesize the 4-dimensional trajectory. The descent trajectory is typically a smooth glide slope starting from the TOD. In real-world operations, ATCs may require a CDA arrival to follow a standard terminal arrival (STAR) procedure for improved predictability or may instruct a shorter ground track to expedite the CDA arrival. Each CDA arrival in the simulation, however, is programmed to follow the ground track of the step-down

trajectory recorded in the ASDI data. In doing this we ensured that the estimated fuel savings is attributed to the CDA instead of efficient rerouting. Because of the difference between the nominal speed profile and the recorded speed profile, the arrival time at the waypoints is changed for the simulated CDA aircraft, resulting in a loss of the original inter-arrival spacing. This scenario, however, is designed to compare with Scenario 1 to measure the fuel savings because of CDA only; conflicts are consequently ignored.

Scenario 3, CDAs with delays: This scenario is similar to Scenario 2, but the flights are rescheduled to arrive at their CDA's TODs to avoid conflicts that are predicted to happen during the descent. The delays for conflict avoidance are absorbed in the en route phase so that the nominal speed profiles are not broken by tactical maneuvers. As a result, the descent profile in Scenario 3 is the same as that in Scenario 2. By comparing the fuel profiles between Scenario 3 and Scenario 2, the fuel burn because of delays can be estimated.

CDA traffic is synthesized using FACET [Bilimoria et al., 2000]. FACET can be configured to run in either PLAYBACK mode or SIMULATION mode. In PLAYBACK mode FACET replays the traffic as recorded in the ASDI data, producing Scenario 1. In SIMULATION mode FACET creates aircraft upon detecting new flights in the data stream and navigates the aircraft using a built-in aircraft performance model based on flight intent information. The descent trajectory is obtained by integrating the nominal descent speed profile along the ground track distance. The aircraft performance model takes several basic constraints into account, such as a CAS of 250 knots below 10,000 ft MSL, acceleration/deceleration limits for civil flights, and a climb/descent rate associated with the particular aircraft type. Airspace constraints, like altitude and speed constraints at a particular arrival fix, are not enforced in the simulation. Arrival procedures must be carefully redesigned to pave the way for CDA deployments, like the DIRTY RNAV STAR described in Johnson [2009].

In addition to the functional simulation components in FACET, the following treatments of data were implemented to create comparable scenarios:

Cruise altitude: Observing the ASDI data, it is often seen that a flight changes its altitude around the TOD, which could be because of data errors caused by radar noise or tactic flight maneuvers. Either one may cause ambiguity in identifying the true cruise altitude. As this study concerns the fairness of fuel comparison more than fidelity of trajectory synthesis, the target cruise altitude is set to be the altitude of observed TOD in the simulation. As such, occasional differences between the target cruise altitude and the observed cruise altitude have no influence on the estimation of fuel savings. Figure 1(a) shows the observed step-down trajectories and their CDA counterparts.

Cruise speed: Similarly, the observed ground speed of an aircraft is not always a constant during cruise. Programming the simulated aircraft to follow exactly the observed speed profile is infeasible in the FACET simulation, as frequent changes in cruise speed increases uncertainties in the TOD location, which results in incomplete descent trajectories. To avoid this problem, the cruise speeds of individual simulated aircraft were

set to be equal to the average cruise speed observed in the corresponding step-down trajectory.

Wind speed: To compute an aircraft's fuel burn, its true airspeed (TAS) is required. But ASDI data only include ground speed. To calculate the TAS, wind speed is needed. FACET provides an interface for weather data derived from the National Center for Environmental Prediction, allowing wind vectors to be read from the RUC-2 at any waypoint for a given time. Figure 1(b) is a snapshot of the RUC 2 wind vectors.

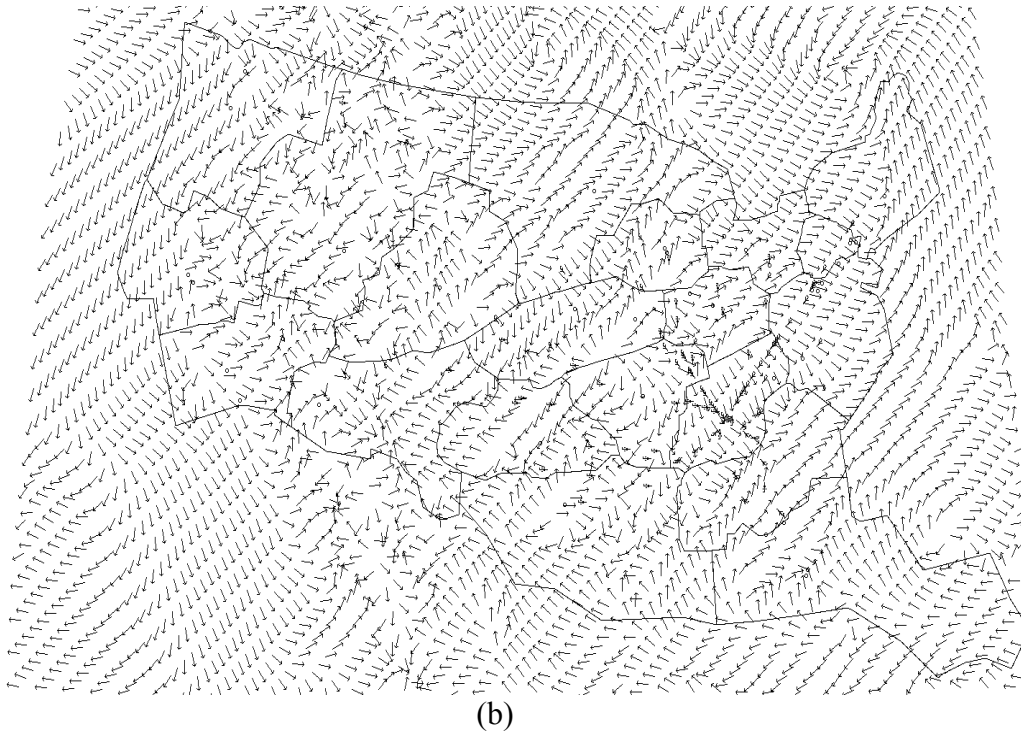
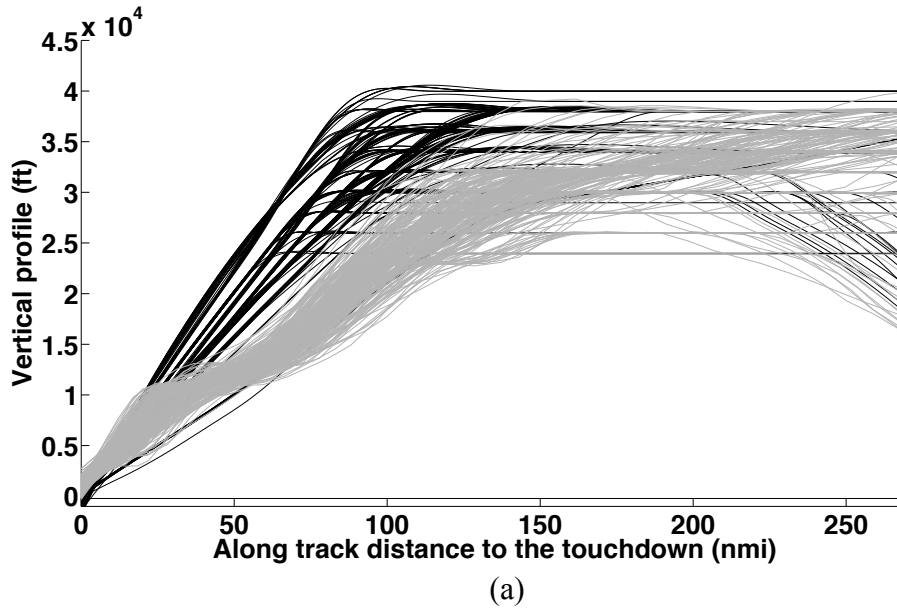


Figure 1. (a) Radar recorded step-down trajectories (gray lines) and FACET simulated CDA trajectories (black lines) along ERLIN NINE STAR into ATL on October 1, 2011. (b) FACET simulation with the corresponding 40-km RUC 2 1-hour wind forecast model.

FUEL MODEL

To estimate the fuel benefits for a wide range of aircraft types, EUROCONTROL's Base of Aircraft Data (BADA) was used [EUROCONTROL, 2011]. BADA v3.9 provides

direct performance data for nearly 117 aircraft models together with an equivalent aircraft type mapping for over 1,000 models. As a result, the majority of aircraft recorded in the ASDI data can be mapped to an appropriate aircraft performance data set in the BADA database. Senzig et al. [2009] reported that fuel estimation based on BADA may deviate from recorded flight data by up to 22.3% below 3,000 ft above field elevation. Using an improved fuel model may reach an accuracy of $\pm 5\%$. The parameters, however, are not publicly available. Therefore, this study still sticks to BADA, which is widely accepted in air traffic management research.

As detailed in the BADA v3.9 user manual, the fuel calculation is strongly related to the aircraft configuration, which corresponds to one of the six flight phases: takeoff, climb, cruise, descent, approach and landing. Unfortunately, the time course of configurations for each aircraft is not recorded in the ASDI data. The configurations must be estimated by comparing the flight altitude and speed with a set of thresholds specified by the BADA. For brevity, we highlight only the basic components and assumptions used for CDA fuel estimation; readers can refer BADA v3.9 user manual for detailed derivation.

The fuel model is termed *Thrust Specific Fuel Consumption* in the BADA. Engine type determines the fuel calculation. The fuel flow rate (f_{nom}) of a piston engine is approximated by a set of constants, while that of jet and turboprop engines are a function of thrust (Thr) given by:

$$f_{nom} = \eta \times Thr \quad (1)$$

where coefficient η is a function of true airspeed V_{TAS} . The thrust Thr and drag D are linked by the total energy model derived from the work-energy theorem:

$$(Thr - D) \cdot V_{TAS} = mgh - mV_{TAS}\dot{V}_{TAS} \quad (2)$$

The true airspeed V_{TAS} and vertical speed \dot{h} can be obtained from the ASDI data or FACET simulations, and the drag D is given by:

$$D = \frac{C_D \cdot \rho \cdot V_{TAS}^2 \cdot S}{2} \quad (3)$$

where ρ is the air density, and S is the wing reference area. The drag coefficient C_D is a function of configurations. Equation (1) is valid for all flight phases except for idle-thrust descent and cruise. Ideally, an aircraft flies with idle thrust (i.e., $Thr = 0$) during the course of CDA. At idle thrust, the fuel flow rate is at a minimum level:

$$f_{min} = C_{f3} \left(1 - \frac{H_p}{C_{f4}}\right) \quad (4)$$

where H_p is the pressure altitude, and C_{f3} and C_{f4} are aircraft specific coefficients. For cruise, the fuel flow rate is adjusted by a factor C_{fcr} :

$$f_{cr} = C_{fcr} \times f_{nom} \quad (5)$$

Whenever equation (1) or (5) yields a value lower than f_{min} , f_{min} should be used.

The estimated fuel profile of a B737 aircraft is illustrated in Figure 2. In the conventional step-down the aircraft begins descending approximately 150 nautical miles (nmi) from touch down along the ground track, then levels off at 12,000 ft MSL. In the CDA

simulation, following the nominal descent speed profile, the aircraft begins descending with an almost constant gradient about 80 nmi from touch down along the ground track. The fuel efficiency of CDA is attributed to removing the low altitude level off. In addition, the CDA keeps the aircraft flying at cruise speed for longer, thus decreasing the flight time. To make the difference perceptible, the fuel flow rate is expressed in kilogram per unit distance. Fuel flow rate increases when the aircraft levels off at low altitude when trying to maintain the same speed.

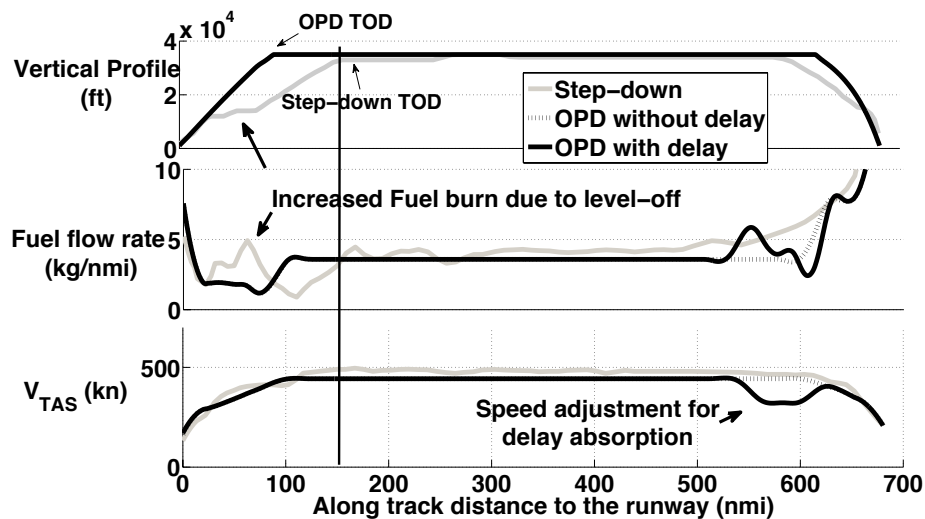


Figure 2. The vertical profile, fuel flow rate, and ground speed of a B737 arrival.

In this paper, we not only examine the fuel burn in the descent phase, but also evaluate the fuel burn because of delays. To make the quantities distinguishable, we introduce two categories of fuel savings:

Gross fuel savings: To compare fuel burn, the starting point of fuel calculation must be carefully defined. As depicted in Figure 2, we count the fuel burn starting from the step-down TOD for both the step-down trajectory and the CDA trajectory, where the fuel burn difference to the left of the vertical line in Figure 2 is the fuel savings because of CDA. Since we simulate all the conflict resolutions for CDA traffic in the cruise phase only, the savings by this definition are solely a consequence of replacing the step-down approach with the CDA approach.

Net fuel savings: This is the benefit accounting for the cost of conflict avoidance, obtained by subtracting the fuel burn for delay absorption from the gross fuel savings. In the CDA simulation with delays, as shown in Figure 2, the aircraft slows down for a while once it reaches the cruise altitude to absorb delays, then it resumes its original cruise speed. The change of fuel burn during this maneuver is because of conflict avoidance.

CONFLICT-FREE CDAS AND DELAY ABSORPTION

When simulating CDAs without delays (non-deconflicted), inter-arrival spacing may be lost because of the change of vertical and speed profiles. Of course, such simulations are

unrealistic, since air traffic controllers would ensure proper separation between arrivals. Re-establishing proper separation involves having the simulated arrivals delay prior to TOD, during cruise, so that the subsequent aircraft trajectories are conflict-free.

This delay can be accomplished in a number of ways. CDAs are largely enabled by advanced onboard FMS and ground automation systems that communicate via data-link [Coppenger et al., 2012]. Given the wind forecast, temperature, pressure, and planned arrival route, the ground-based system can compute a conflict-free CDA arrival route for each arriving aircraft. Once uploaded to the flight deck, a set of descent advisories direct the aircraft to fly a CDA with no additional pilot inputs and ATC intervention. Hence, the success of CDA implementation relies heavily on strategic planning. To simulate the conflict-free CDA traffic, this study employs a McTMA-like algorithm to provide a time-based metering (TBM) [Landry et al., 2003], which is a technique to stretch out arrival demand that exceeds national airspace resources by deconflicting the initial schedule and creating deconflicted times. These times are so-called “scheduled times of arrival” (STAs) that intend to delay aircraft in Air Route Traffic Control Center (ARTCCs). As the McTMA system is designed for multiple-center scheduling, its coverage can radiate to airspace that is sufficiently large to cover all the descent trajectories [Landry et al., 2012].

To meet the STAs computed by the McTMA algorithm, aircraft must take appropriate actions to absorb en route delays. Maneuvers used to absorb airborne delays mainly involve path stretching, speed change, and airborne holding. While these maneuvers necessitate the need for power, a CDA arrival usually avoids deviating from its preferred settings once it is cleared for descending. Therefore, aircraft preferably absorb delays before hitting the TOD.

Delay absorption is a key factor that causes variation in fuel efficiency. To understand its impact, we created sub-scenarios in the Scenario 3, where we varied the delay absorption in two dimensions. First, we used different separation minima to examine the influence of increased separation. Ren’s research shows that the uncertainty of arrival time increases as flights approach runway threshold [Ren and Clarke, 2007]. As a result, a separation buffer is necessary when spacing CDA arrivals. Second, we used different single maneuvers to absorb delays. Although real-world operations usually adopt a combination of maneuvers to optimize the cost, it is difficult to emulate the operations in FACET. Alternatively, we simulated each single maneuver to estimate the bounds. The implementation of each maneuver is described below.

Scenario 3(1): Speed change. Changing the cruise speed is the cheapest way to adjust the arrival time as it does not change the path. The new cruise speed is computed based on required delays. As the focus here is the fuel efficiency, we first target the fuel-optimal speed. Fuel-optimal speed is a cruise speed that leads to least fuel under International Standard Atmosphere at a given altitude for a particular aircraft type based on the Total Energy Model [Jin et al., 2013]. If the fuel-optimal cruise speed is infeasible, we try to find a feasible solution by releasing fuel constraints. The solution is still constrained by the minimum cruise speed and the maximum distance-to-fly. If no feasible

solution is found, path stretching is used to absorb the delay. The algorithm is detailed in the Appendix.

Scenario 3(2): Path stretching. Extending the lateral flight path is another effective means to absorb delays [Erzberger et al., 2010], which typically involves a series of heading change to make the aircraft temporarily deviate from their original planned paths and turn back later. In the simulation, the aircraft were programmed to maintain their original cruise speeds when executing path stretching.

Scenario 3(3): Air holding. Holding patterns are typically used to absorb large delays and when there is a sudden need to reduce the injection of air traffic into the airport terminal area. In congested traffic the ATC may vector an arriving aircraft to a designated fix for further clearance for approach and landing. With a racetrack pattern a standard holding pattern can absorb at least 4 minutes for a complete hold, with 2 minutes for inbound and outbound legs and 1 minute for each 180-degree turn [FAA-H-8083-15A, 2009]. Although air holding is less precise in delay absorption than path stretching or speed change, it is interesting to compare its fuel efficiency with the others. In this sub-scenario we assume that the delayed aircraft is held in an upstream fix before its TODs for delay absorption. The FAA specified the maximum holding speed (shown in Table 1) for civil aircraft to restrict the holding pattern within the controlled airspace. As a result, the delayed aircraft must adjust its speed to comply with the airspeed limit when arriving at the holding fix and resume its original airspeed when leaving the fix.

Table 1. FAA Maximum Holding Speed

Altitude Mean Sea Level (ft)	Indicated Airspeed (kn)
Up to 6,000	200
6,000 – 14,000	230
14,000 and above	265

SIMULATION RESULTS AND SENSITIVITY STUDY

Among the 16,913 aircraft identified in the ASDI data, 1,342 aircraft were labeled unrecognizable aircraft models. To preserve the traffic density, these aircraft were replaced with aircraft types that are common at their cruise altitudes. As described previously, by comparing Scenarios 1 and 2, we obtained the gross fuel savings. By comparing the sub-scenarios of Scenarios 3 and 2, we obtained the fuel consumption because of delay absorption.

The variability identified through the case study falls mainly into two categories. The first category is traffic relevant, which influences the en route fuel burn. The second category is traffic irrelevant, which influences the gross fuel savings.

Traffic relevant factors

Table 2 summarizes the fuel savings. In Scenario 2, where delay absorption was not enforced, the gross fuel savings of 2,783 tons set the upper bound that CDAs can achieve. In Scenario 3, the separation minima and delay absorption maneuver were varied to examine the sensitivity of fuel benefits to the variability sources. The wake turbulence separation minima regulated in the Instrument Flight Rules ranges from 2.5 to 5 nmi, and Ren’s research suggests a buffer ranging from 0.26 to 0.75 nmi to account for uncertainty [Ren and Clarke, 2008]. Therefore, we chose three integers as the required separations in the simulations. The savings in each entry are the net fuel savings accompanied by the ratio to the gross fuel savings in the brackets. It is not a surprise that the savings decreased as larger separation was enforced. Among the three maneuvers, speed changes preserve the most savings among the three types of maneuvers. This savings is because of the decrease in cruise speed. When cruising at high speed, flights are experiencing high drag as indicated by equation (3). Decreasing speed will decrease the drag, thus less thrust is needed. These factors would translate into a lower fuel flow rate. As a result, speed change absorbs the extended flight time at a lower fuel cost in comparison to air holding and path stretching.

Table 2. Evaluation Matrix Using Different Separation Minima and Delay Absorption Maneuvers. (Fuel savings (in tons) are drawn from the two-week traffic.)

Separation minima		3NM	5NM	6NM
Scenario 2 (gross fuel savings)		2,783	2,783	2,783
Scenario 3 (net fuel savings)	Speed	2,382 (86%)	2,410 (83%)	1,947 (70%)
	Holding	2,191 (79%)	2,030 (73%)	1,791 (64%)
	Stretching	2,164 (78%)	2,130 (77%)	1,692 (60%)

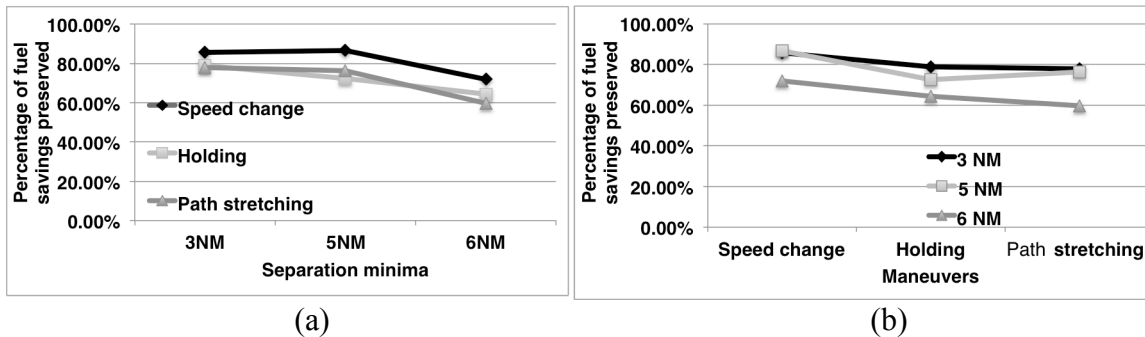


Figure 3. (a) Preserved fuel savings versus separation minima. (b) Preserved fuel savings versus maneuvers.

Figure 3 visualizes the sensitivity of fuel savings to different parameters, where higher numbers indicate more fuel savings preserved and, therefore, is better. The slopes of the lines in subfigures (a) and (b) indicate that the fuel savings are more sensitive to the separation minima than to the maneuvers. For the same separation minima, the variation of savings is less than 10% when maneuvers change. In contrast, the variation changes up to 19% for the same maneuvers when separation minima change.

Presenting the statistic by days enables a close examination on the relationship between arrival demand, delays and fuel savings. Table 3 summarizes the daily statistics drawn from CDA simulations with separation minima equal to 5 nmi, and Figure 4 visualizes the numbers listed in Table 3 on a per flight basis.

Table 3. Daily Operational Statistics and Fuel Savings (in tons) Associated with Delay Absorption Maneuvers (separation = 5 nmi).

Date	Arrival (flight)	Delays (min)	Gross savings	Net saving (holding)	Net saving (stretching)	Net saving (speed)
10/1/11	1,009	832	149	129	134	141
10/2/11	1,186	1,168	171	124	133	150
10/3/11	1,263	1,647	209	144	155	179
10/4/11	1,195	1,506	180	122	131	152
10/5/11	1,236	1,402	223	166	177	197
10/6/11	1,291	1,603	227	161	175	197
10/7/11	1,277	1,834	188	126	129	154
10/8/11	980	1,099	169	124	133	149
10/9/11	1,177	1,210	192	155	152	170
10/10/11	1,303	1,717	206	148	151	174
10/11/11	1,213	1,603	205	155	153	175
10/12/11	1,247	1,475	225	161	177	198
10/13/11	1,280	1,492	204	144	155	176
10/14/11	1,256	1,781	236	172	177	203
Total	16,913	20,369	2,783	2,030	2,130	2,410

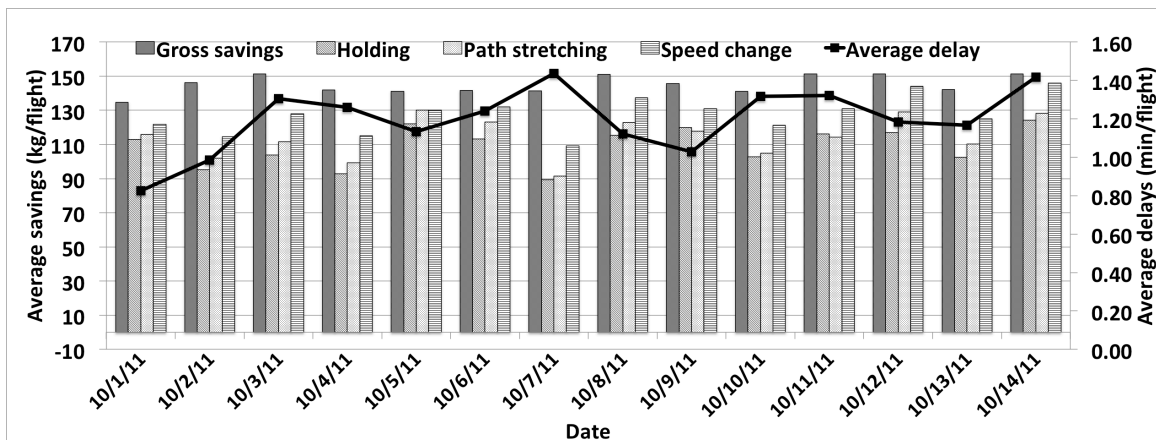


Figure 4. Average fuel savings on each day.

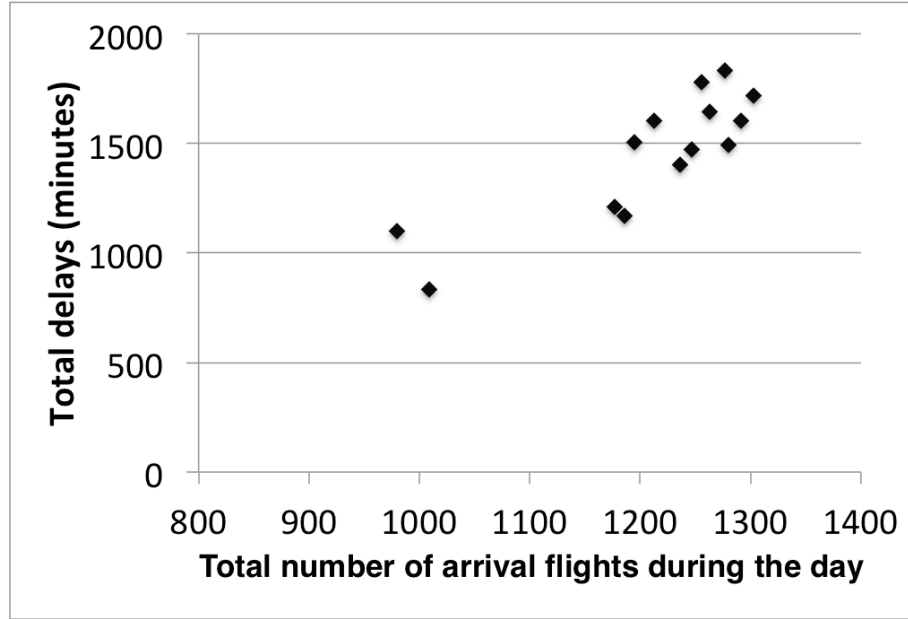


Figure 5. Total delays increases as traffic demand increases.

The average gross fuel savings across the days is 147 kg/flight. The average net fuel savings are 110 kg/flight, 115 kg/flight, and 123 kg/flight for air holding, path stretching, and speed change, respectively. The average delay across the days is 1.2 minutes/flight with a standard deviation of 0.4 minutes/flight. The variation of delays is because of the varying traffic demand. Figure 5 shows that the total delays increase as the traffic volume increases. This variation is also reflected in the amount of reduction of fuel savings. On October 7th when the arriving aircraft were subject to an average delay of 1.4 minutes, 28%~42% of the gross fuel savings were lost, depending on maneuver types. On October 1st when the arriving aircraft were subject to an average delay of 0.8 minutes, only 9%~16% of the gross fuel savings are lost. This observation indicates that the savings reduction is closely related to the average delays, which is evident in Figure 6. The distribution of the data suggests a linear relationship between savings reduction and delays. Linear regression yields:

$$\text{Avg savings reduction (kg/AC)} = \begin{cases} 31.25 \times \text{Avg delays (min)}, R^2 = 0.86, \text{ path stretching} \\ 34.36 \times \text{Avg delays (min)}, R^2 = 0.93, \text{ air holding} \\ 18.07 \times \text{Avg delays (min)}, R^2 = 0.93, \text{ speed change} \end{cases} \quad (6)$$

The implication of Equation (6) is that whenever the average delay increases by 1 minute per flight, the average fuel savings decrease by 18.07~34.36 kg per flight, depending on delay absorption maneuvers.

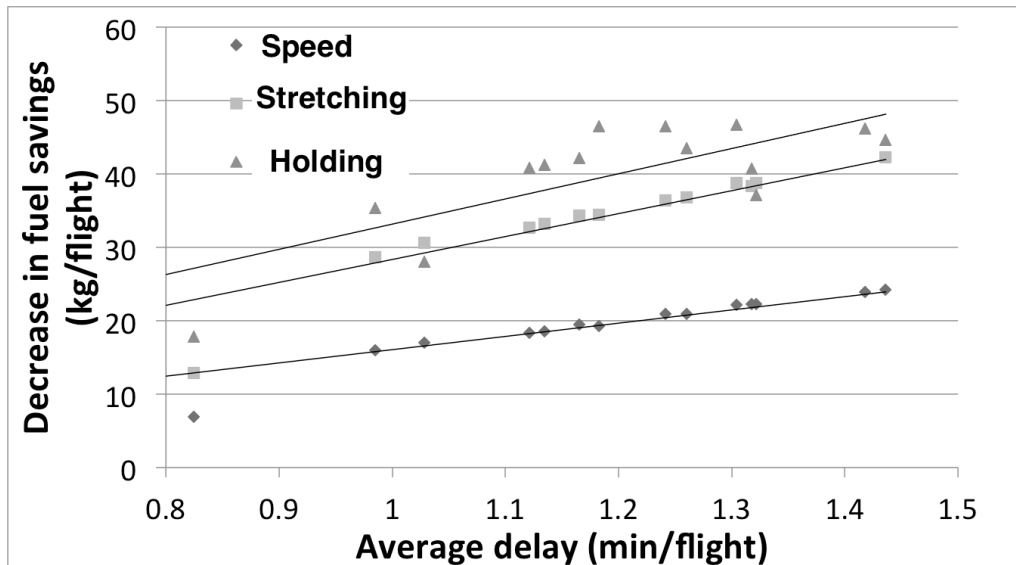


Figure 6. Linear relationship between average delay and average fuel savings reduction.

Traffic irrelevant factors

An aircraft's fuel consumption is related to the aircraft weight m (see Equation (2)). Since the takeoff weight is unavailable in the ASDI data, we use the reference mass recommended by the BADA v3.9. Figure 7 shows the average gross fuel savings for each weight group. As expected, the heavier the aircraft, the higher the gross fuel savings.

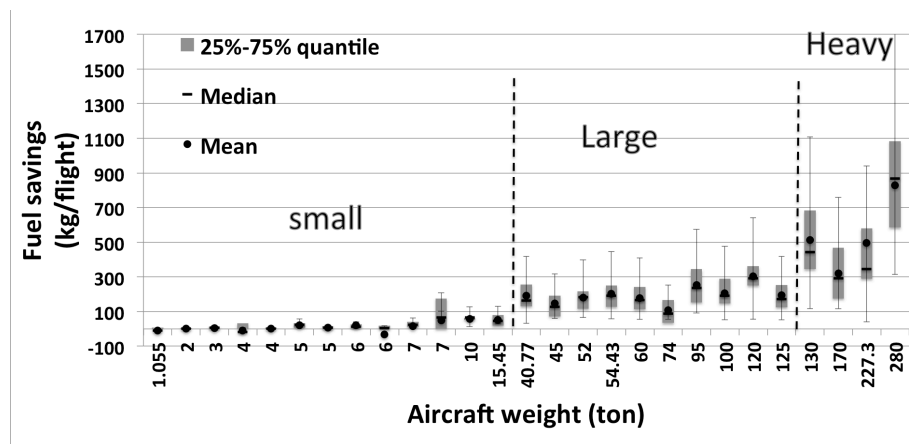


Figure 7. Gross fuel savings for different aircraft weight groups.

For an individual aircraft, its weight determines the scale of savings. For the fleet mix as a whole, however, the composition of weight categories influences the average saving efficiency. In Figure 8 (a) the daily total gross fuel savings are decomposed to show the contribution of each weight category. The Large group and Heavy group are the major contributors to the total fuel savings, with slightly interchanged percentages over days. Figure 8 (b) shows the composition of weight categories on each day. The Large group and the Heavy group account for roughly 43% and 33% of the arrivals, respectively. The

trend lines suggest that the Large group and the Small group have slight increases in the percentages while the Heavy group experiences a decrease as the daily arrival demand increases. The percentage changes in Figure 8 (a) and (b) suggest that the fuel efficiency of the Large group is actually decreasing. As the largest arrival body in the fleet mix, its efficiency dominates the overall average fuel efficiency.

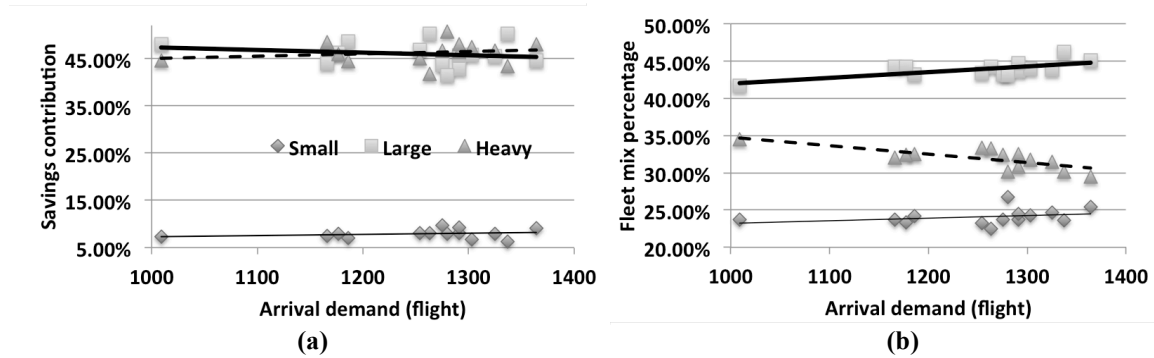


Figure 8. (a) Normalized contribution to the fuel savings for each weight category. (b) Composition of weight categories in the fleet mix.

The gross fuel savings are also closely related to the step-down itself. Once the speed profile is chosen, the vertical profile a particular aircraft model will fly is almost fixed. As a result, the CDAs of that aircraft model are similar except for different initial descent altitudes and TOD positions. Therefore, the “savings” amount is determined by the step-down trajectories, which could have greater degree of variations. Figure 9 presents the gross fuel savings versus the number of level-offs observed in the step-down trajectories. The majority of arriving aircraft execute one or two level-offs in the descent phase. Obviously, when the aircraft fly more level-offs, more fuel is burned because of frequent throttle up and down. Thus, eliminating those level-offs saves a significant amount of fuel.

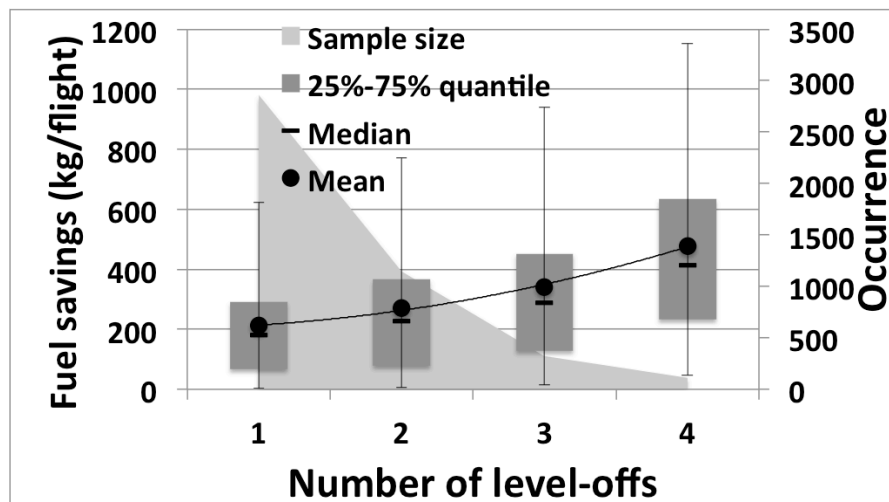


Figure 9. Gross fuel savings as a function of number of level-offs in the observed step-down trajectory.

DISCUSSION

Because of the lack of fuel data from airlines, the precision of the estimation is difficult to know. To validate the credibility of this simulation-based evaluation, a cross-study comparison is made, which aims at ensuring that the fuel burn estimation is consistent with previous studies within a reasonable range of discrepancy. Roughly, the International Air Transportation Association (IATA) reported 50 ~ 200 kg of gross fuel savings per flight [IATA], while the estimate by this study is 147 kg/flight. A cross-study comparison is shown in Table 4. The chosen studies are comparative in a sense that all of the studies employ BADA model for fuel estimation and metering actions are incorporated in the evaluations. The statistic is given as ranges to account for the variability of traffic scenario and methodology in different studies. Overall, the average net fuel savings of 110~123 kg/flight by this study is within or close to the ranges reported by the previous studies. In addition, Robinson et al. [2010] reported a reduction of 45 kg/flight due to traffic congestion at ATL, in comparison with a reduction of 23~36 kg/flight by this study. This is because a speed adjustment was applied which results in higher fuel flow rate in Robinson's study. Coppenbarger et al. [2009] suggested a 25% savings reduction due to heavy traffic, equivalent to 27.5~365.5 kg/flight. And Shresta et al. [2009] reported a more aggressive reduction of 85%. Despite the large variation in these estimates, all of these studies agree on the fact that increased traffic demand will negatively and significantly impact the benefits, which has been statistically quantified by this study.

Table 4. Cross-study Comparison of Average Fuel Savings with ATC Control

Published Study	Airport	Savings (kg/flight)
Robinson et al., 2010	ATL	25~105
Coppenbarger et al., 2009	SFO	110-1462
Shresta et al., 2009	DEN	60~132
Cao et al., 2013	ATL	110~123

Some planned air traffic management system developments may help mitigate such negative impacts. The key is to reduce delays that rely heavily on strategic planning. A combination of maneuvers grants greater flexibility in solving near-term and long-term conflict. The Efficient Descent Advisor (EDA), under development by NASA, is able to calculate dynamically the optimal arrival path with a combination of cruise-speed advisory, descent-speed advisory, and path adjustment [Coppenbarger et al., 2012], better leveraging delay cost and system efficiency. Furthermore, the integration of ground automation and onboard FMS, typically enabled by data link, paves the way for precise execution of strategic planning. Working together with TMA, the current EDA is able to generate a predicted trajectory that is uploaded to the FMS for execution with 92% accuracy improvement. As such, the uncertainty of Scheduled Time of Arrival at metering fix is dramatically reduced. The need for large separation is thus less imperative, which enhances the operational feasibility of CDAs.

CONCLUSION

This paper investigates the potential fuel benefits of Continuous Descent Approach under traffic conditions based on air traffic simulation and BADA fuel model. The relationship between delays and benefits reduction is examined closely. Simulation results reveal that the removal of level flights in the descent phase saves 147 kg of fuel per flight. Delays resulting from the additional need for deconfliction, however, lead to a reduction of 23~42 kg of fuel per flight. Moreover, the potential fuel savings are sensitive to the separation minima. With the increase of separation the savings almost linearly decrease. Compared to separation minima, the delay absorption maneuvers have a minor impact on the savings. In addition, the amount of fuel savings is closely related to the aircraft weight category. Enabling Large or Heavy aircraft to engage in CDA will achieve higher benefits. The average savings at the airport are also related to the composition of weight category. The fuel efficiency of Large and Heavy aircraft dominates the whole fuel efficiency at an airport.

Since air traffic involves various random human decisions and is impacted by multidimensional factors, numeric results based on simulations, which are often limited by availability of data and simulation setup, are no more than an approximation to reality. In this study, the BADA may introduce errors in fuel estimate in the terminal airspace. Also, air traffic controllers might compress separations as flights approach the destination airport. Using a fixed separation minima to space flights may result in excessive separations and, thus, underestimate the net fuel savings. The simulations in this work are unable to simulate variant separations along descent trajectories. The simulations, however, use different separation minima to approximate the bounds of potential fuel savings, which is intended to provide insights into the scale of savings.

ACKNOWLEDGMENT

This research is sponsored by the FAA through the National Center of Excellence for Aviation Operations Research (NEXTOR II) under Delivery Order #8. We are grateful to Mr. Richard Coppenbarger from NASA's Ames Research Center who shared his valuable insight on the modeling and simulation of Continuous Descent Approach.

ASDI	Aircraft Situation Display to Industry
3DPAM	Three-dimensional path arrival management
ARTCC	Air Route Traffic Control Center
ATC	air traffic controller
ATL	Hartfield-Jackson International Airport
BADA	Base of Aircraft Data
CAS	calibrated airspeed
CDA	continuous descent approach
CD&R	conflict detection and resolution
EDA	Efficient Descent Advisor
FACET	Future ATM Concepts Evaluation Tool
FAA	Federal Aviation Administration
FMS	flight management system
IATA	International Air Transportation Association

NAS	National Airspace System
McTMA	Multi-center Traffic Management Advisor
MSL	mean sea level
NASA	National Aeronautics and Space Administration
NEXTOR II	National Center of Excellence for Aviation Operations Research
NOAA	National Oceanic and Atmospheric Administration
OPD	Optimized Profile Descent
OEP	Operational Evolution Partnership
STA	scheduled times of arrival
STAR	standard terminal arrival
TAS	true airspeed
TBM	time-based metering
OPTIMAL and Landing	Optimized Procedures and Techniques for Improvement of Approach
PARTNER	Partnership for Air Transportation Noise and Emission Reduction
TRACON	Terminal Radar Approach Control
TOD	top-of-descent
RUC2	Rapid Update Cycle version 2
TFMS	Traffic Flow Management System
TOD	top-of-descent

REFERENCES

Bilimoria, K., Sridhar, B., Chatterji, G., Sheth, K., and Grabbe, S. (2000), "FACET: Future ATM Concepts Evaluation Tool," *3rd USA/Europe Air Traffic Management R&D Seminar*, Napoli, Italy, 13-16 June.

Cao, Y., Kotegawa, T., Sun, D., DeLaurentis, D., Post, J. (2011) "Evaluation of Continuous Descent Approach as a Standard Terminal Airspace Operation," *9th USA/Europe Air Traffic Management Research and Development Seminar*. Berlin, Germany, June 14-17, 2011.

Clarke, J. B. (2006), "Development, design, and flight test evaluation of a continuous descent approach procedure for nighttime operation at Louisville International Airport," Report No. PARTNER-COE-2005-02, January 9.

Clarke, J. B., Ho, N. T., Ren, L., Brown J. A., Elmer, K. R., Tong, K., and Wat, J. K. (2004), "Continuous Descent Approach: Design and Flight Test for Louisville International Airport," *Journal of Aircraft*, Vol. 41, No. 5, September–October.

Coppenbarger, R., Mead, R., Sweet, D. (2009), "Field Evaluation of the Tailored Arrivals Concept for Datalink-Enabled Continuous Descent Approach," *Journal of Aircraft*, Vol. 46, No. 4, pp. 1200-1209.

Coppenbarger, R., Hayashi, M., Nagle, G., Sweet, D., Salcido, R. (2012), "The Efficient Descent Advisor: Technology Validation and Transition," *12th AIAA Aviation Technology, Integration, and Operations (ATIO) Conference*, 17-19 September, Indianapolis, IN.

de Muynck, R. J. (2007), "D2.2-1 Aircraft procedures definition-ACDA," Document ID: WP2-NLR-022 -V1.2-TW-CO. URL: <http://www.optimal.isdefe.es/public/publications/CDA.html>

Erzberger, H., Lauderdale, T. A., Chu, Y-C (2010), "Automated conflict resolution, arrival management, and weather avoidance for air traffic management," *27th International Congress of the Aeronautical Science, Nice, France*.

FAA-H-8083-15A (2009), Instrument Flying Handbook, Chapter 10. http://www.faa.gov/library/manuals/aviation/instrument_flying_handbook/media/FAA-H-8083-15A%20-%20Chapter%2010.pdf

FAA, (2012). http://www.fly.faa.gov/Information/east/ztl/atl/atl_aar.htm

IATA, INFRASTRUCTURE - SAVINGS FUEL "Dive & Drive" vs. Continuous Descent Arrival (CDA). <http://www.iata.org/SiteCollectionDocuments/Documents/InfrastructureSavingFuelCDA Brief.pdf>

- Jin, L., Cao, Y., and Sun, D. (2013), "Investigation into Potential Fuel Savings due to Continuous Descent Approach," *AIAA Journal of Aircraft*, Vol. 50, No. 3, pp. 807-816, May-June.
- Johnson, C. M. (2009), "Human-In-The-Loop (HITL) Simulation and Analysis of Optimized Profile Descent (OPD) Operations at Atlanta," The MITRE Corporation, McLean, VA, Contract DTFA01-01-C-00001 Rep. 093665, November.
- Landry, S., Farley, T., Foster, J., Green, S., Hoang, T., and Wong, G. L. (2003), "Distributed scheduling architecture for multi-center time-based metering." *AIAA Aircraft Technology, Integration and Operations (ATIO) Conference*.
- Landry, S. J., Farley, T., Hoang, T., and Stein, B. (2012), A distributed scheduler for air traffic flow management. *Journal of Scheduling*, 15(5), 537-551.
- Khan, Z., Idris, H., Vivona, R., Woods, S., and Lanier, R. C. (2009) "Ground automation impact on enabling continuous descent in high density operations," *9th AIAA Aviation Technology, Integration, and Operations Conference (ATIO)*, Hilton Head, SC, 21 - 23 September.
- Reynolds, T. G., Ren, L., Clarke, J. B., Burke, A. S., and Green, M. (2005), "History, development and analysis of noise abatement arrival procedures for UK airports," *5th AIAA Aviation, Technology, Integration, and Operations Conference (ATIO)*, Arlington, VA, 26-28 September.
- Ren, L. and Clarke, J. B. (2007), "Separation Analysis Methodology for Designing Area Navigation Arrival Procedures," *Journal of Guidance, Control, and Dynamics*, Vol. 30, No. 5, pp. 1319-1330.
- Ren, L. and Clarke, J. B. (2008), "Flight-Test Evaluation of the Tool for Analysis of Separation and Throughput," *Journal of Aircraft*, Vol. 45, No. 1, pp. 323-332.
- Robinson III, J. E. and Kamgarpour, M. (2010), "Benefits of Continuous Descent Operations in High-Density Terminal Airspace under Scheduling Constraints," *10th AIAA Aviation Technology, Integration, and Operations (ATIO) Conference*, Fort Worth, TX, 13-15 September.
- Senzig, D. A., G. G. Fleming, and R. J. Iovinelli (2009), "Modeling of Terminal Area Airplane Fuel Consumption," *Journal of Aircraft*, Vol. 46, No. 4, July–August.
- Shresta, S., Neskovic, D., and Williams, S. S. (2009), "Analysis of Continuous Descent Benefits and Impacts during Daytime Operations," *Eighth USA/Europe Air Traffic Management Research and Development Seminar (ATM2009)*, Berlin, Germany, June.
- EUROCONTROL (2011), User Manual for the Base of Aircraft Data (BADA) Revision 3.9. URL: http://www.eurocontrol.int/eec/gallery/content/public/document/eec/other_document/2011/EEC-Technical-Report-110308-08.pdf.

White, W. and Clarke, J. P. (2006), "Details and status of CDA procedures at Los Angeles International Airport (LAX)," *CDA Workshop No. 3*, Georgia Institute of Technology, Atlanta, GA, 6-7 September.

Wat, J., Follet, J., Mead, R., Brown, J., Kok, R., Dijkstra, F., and Vermeij, J. (2006), "In service demonstration of advanced arrival techniques at Schiphol Airport," *6th AIAA Aviation Technology, Integration and Operations Conference (ATIO)*, Wichita, KS, 25-27 September.

Wilson, I. and Hafner, F. (2005), "Benefit assessment of using continuous descent approaches at Atlanta," *The 24th Digital Avionics Systems Conference*. Washington, DC, 30 October - 3 November. *We need more information here.*

BIOGRAPHIES

Yi Cao received a bachelor's degree in Instrumentation Science and Engineering in 2006, and a master's degree in Navigation, Guidance and Control in 2009 from Shanghai Jiao Tong University, China. He received a Ph.D. from the School of Aeronautics and Astronautics, Purdue University. His research focuses on modeling, optimization, and simulation, with an emphasis in air traffic flow management.

Li Jin is a graduate student researcher at the Purdue University School of Mechanical Engineering. He received his bachelor's degree in mechanical engineering from Shanghai Jiao Tong University. His research interest lies in air traffic management, with an emphasis on terminal area operation.

Nguyen V. P. Nguyen is currently pursuing his Ph.D. in Industrial Engineering at Purdue University. He received his B.E. in Industrial Systems Engineering at the University of Technology, Vietnam National University, Ho-Chi-Minh City in 2002. From 2002 to 2010, he worked as an instructor at Industrial Systems Engineering Department, University of Technology. His doctoral research is on situation awareness modeling and its application in aviation systems.

Steven Landry is an Associate Professor and Associate Head in the School of Industrial Engineering at Purdue University. He received his Ph.D. in Industrial and Systems Engineering from Georgia Tech in 2004, an S.M. in Aeronautics and Astronautics from MIT in 1999, and a B.S. in Electrical Engineering from WPI in 1987. Prior to Purdue, he was an aerospace engineer at NASA Ames Research Center working on the Multi-Center Traffic Management Advisor system and Automated Airspace Concept. He accumulated more than 2,500 hours as a C-141B pilot with the US Air Force between 1990 and 1997.

Dengfeng Sun received a bachelor's degree in precision instruments and technology from China's Tsinghua University, a master's degree in industrial and systems engineering from the Ohio State University, and a Ph.D. in civil engineering from the University of California-Berkeley. Dr. Sun's research areas include control and optimization, with an emphasis on applications in air traffic flow management, dynamic airspace configuration, and studies for the Next Generation Air Transportation System (NextGen).

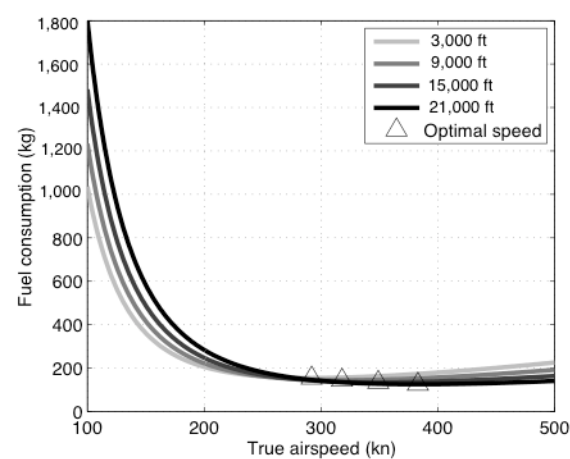
Joseph Post is the Director of Systems Analysis in the Federal Aviation Administration's NextGen organization. He received a bachelor's degree in aeronautics and astronautics from the Massachusetts Institute of Technology, a master's degree in electrical engineering from Yale University, and a master's degree in economics from George Mason University. Mr. Post holds numerous patents in the area of automatic flight control systems and is an instrument-rated pilot.

APPENDIX

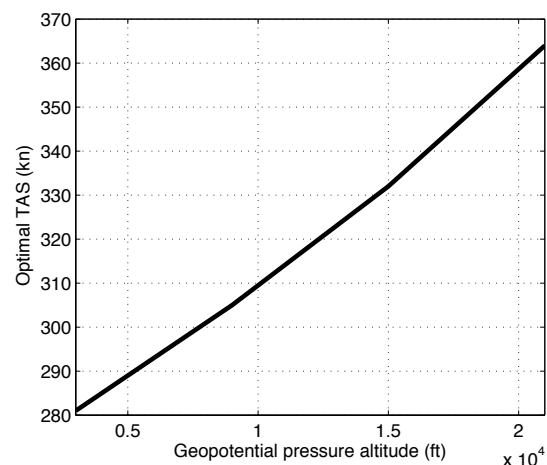
Derivation of en route Speed Change Solution

Speed change solution is a function designed for providing en route speed advisory to meet delay absorption requests without changing ground track. Feasibility of this problem is constrained by three inputs: minimum cruising speed v_{cr_min} of a specific aircraft type, delay to absorb T_{delay} , and ground track distance-to-fly d , which is the ground track distance between the current position of the aircraft and the position of its predicted TOD. If d is long enough, the aircraft will have sufficient space to absorb the delay by cruising at a lower speed. In a co-authored work [Jin et al., 2013], the authors analyzed the relationship between speed profile and fuel efficiency based on BADA under International Standard Atmosphere conditions [EUROCONTROL, 2011]. In a benchmark test, we found that speed has a nonlinear, as well as non-monotonic relationship, with the fuel consumption. Traveling at a higher speed will increase fuel flow rate, but flight time is reduced. These two factors compete, which leads to profiles shown in Figure (a). A speed exists that leads to the least fuel burn at a given altitude. As altitude changes, the fuel-optimal speed changes accordingly, as shown in Figure (b). From an environmental perspective, a flight is supposed to fly at a fuel-optimal speed whenever possible. As a result, the speed adjustment pursues a solution with the following fallback mechanism:

- a) A fuel-optimal speed solution v_{cr_opt} that absorbs the required delay while minimizing fuel burned.
- b) A feasible speed solution v_{cr_fea} that absorbs the required delays.
- c) The distance-to-fly d is too short to absorb the required delay, which means the flight is unable to absorb the given delays even if it cruises at the minimum cruise speed v_{cr_min} , in which case the speed change solution is infeasible.



(a)



(b)

Figure 10 Fuel profile of B747 presented in a benchmark test in [Jin et al., 2013] (a) Fuel consumption by traveling the same distance versus true air speed at different altitudes. (b) Fuel-optimal cruise speed versus altitude.

The key is to identify two thresholds in the fallbacks, d_{opt} and d_{min} . d_{opt} denotes the minimum distance that allows the flight to fly at its fuel-optimal speed to absorb the required delay, and d_{min} denotes the minimum distance that allows the flight to fly at its minimum cruise speed to absorb the required delay. Given that v_{cr_opt} is higher than v_{cr_min} , it is intuitive that $d_{opt} > d_{min}$. The assumption used here is that the flight deviates from its planned cruise speed upon receiving a delay command and resumes the planned cruise speed for not changing its planned descent speed profile so that its descent trajectory profile will be unchanged for subsequent de-confliction.

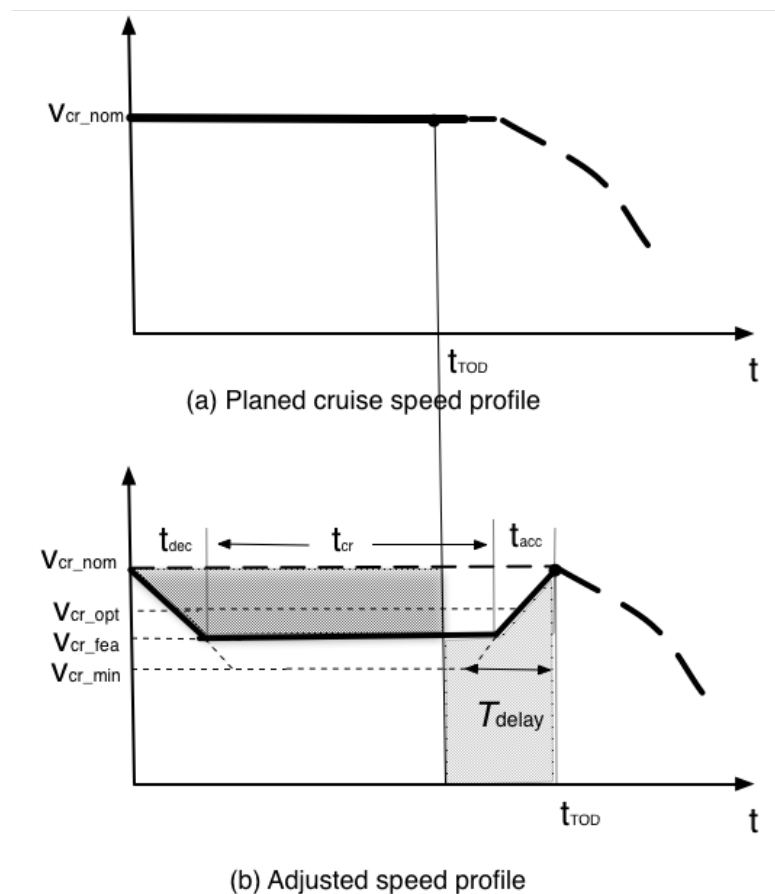


Figure A-2. Speed change profiles constrained by delay T_{delay} and distance-to-fly d , resulting in three possible outputs.

The adjusted speed profile is shown in Figure (b). For simplicity, the aircraft is assumed to change speed using constant acceleration and deceleration a_{\max} , which is specified in BADA for civil flight. Let t_{dec} , t_{cr} and t_{acc} denote the time during which the aircraft decelerates, cruises at a lower cruise speed, and accelerates respectively. And let v_{cr_nom} denotes the original cruise speed. The solution would be a speed v_{cr_fea} bounded by v_{cr_opt} and v_{cr_min} , if the distance-to-fly d permits.

From Figure (a), it is easy to calculate the time for constant deceleration and acceleration:

$$t_{dec} = t_{acc} = \frac{v_{cr_nom} - v_{cr_fea}}{a_{\max}} \quad (1)$$

Since the distance-to-fly d is unchanged, the flight must catch up during the delay period. As a result, the shade areas must be equal. which gives the following equation:

$$\left(\frac{t_{dec}}{2} + t_{cr} + t_{acc} - T_{delay}\right)(v_{cr_nom} - v_{cr_fea}) = T_{delay} v_{cr_fea} + t_{acc} (v_{cr_nom} - v_{cr_fea}) \quad (2)$$

The area enveloped by the adjusted speed profile is the distance to fly:

$$d = v_{cr_nom} (t_{cr} + t_{dec} + t_{acc}) - \frac{(2t_{cr} + t_{dec} + t_{acc})(v_{cr_nom} - v_{cr_fea})}{2} \quad (3)$$

Replacing t_{dec} and t_{acc} with Equation (1) in Equation (2), t_{cr} can be resolved. Replacing v_{cr_fea} with v_{cr_opt} or v_{cr_min} in Equation (3), the distance is expressed as a function of known parameters and correspond to d_{opt} and d_{min} respectively:

$$d_{opt} = \frac{(v_{cr_nom} - v_{cr_opt})(2v_{cr_nom} + v_{cr_opt})}{2a_{\max}} + \frac{T_{delay} v_{cr_nom} v_{cr_opt}}{v_{cr_nom} - v_{cr_opt}} \quad (4)$$

Once d_{opt} and d_{min} are resolved, the boundaries for the fallbacks are obtained. If

$d_{min} \leq d \leq d_{opt}$, which means the current distance-to-fly is not long enough to absorb the delay by v_{cr_opt} , so it needs to find a speed v_{cr_fea} between v_{cr_min} and v_{cr_opt} , which can be derived by resolving Equation (3).

In summary, the speed change solution is given by the following logic:

$$\left\{ \begin{array}{ll} d \geq d_{opt} & \text{output } v_{cr_opt} \\ d_{opt} > d \geq d_{min} & \text{output } v_{cr_fea} \\ d < d_{min} & \text{infeasible} \end{array} \right.$$